

FINITE ELEMENT MODELS OF LITHOSPHERIC FLEXURE AND VOLCANIC SPREADING AT OLYMPUS MONS, MARS. S. Musiol¹ and G. Neukum¹, ¹Freie Universität Berlin, Institute of Geological Sciences, Planetary Sciences and Remote Sensing, Malteserstr. 74-100, 12249 Berlin, Germany (stefanie.musiol@fu-berlin.de).

Introduction: Olympus Mons is a basaltic shield volcano on the Martian surface with a height of 22 km, an extent of 840×640 km including recent lava flows, and an average flank slope of 5° [1]. Noticeable features of Olympus Mons are a central caldera complex, upper-flank terraces resembling thrust faults [2,3], an up to 8 km high circumferential scarp, and several aureole lobes with runout distances in excess of 700 km. Further, a flexural moat that is filled with lava surrounds Olympus Mons [4,5].

The scarp is obvious from a break in slope at the lower flanks, where the flank slope increases to $30-40^\circ$. [6,7] interpret the scarp as a product of basal thrusting due to volcanic spreading. The widespread aureole deposits are genetically associated with individual scarp segments, and could have been caused by mass movement [8,9,10].

The goal of this investigation is to understand the role of lithospheric flexure and volcanic spreading in the evolution of Olympus Mons. For this purpose the deformation of the volcanic cone under Mars gravity is investigated with numerical models.

Model: Axisymmetric finite element models of volcanic loading of an elastoplastic cone on top of an elastoplastic lithosphere overlying a viscoelastic mantle were performed.

The model dimensions are 1500 km width and depth, respectively, to minimize the influence of model boundaries. The initial volcano height is 40 km to match the observed height after flexure. The volcano radius is 400 km, larger than the observed distance from volcano center to scarp of about 300 km, because the state of the volcano prior to failure and scarp formation is to be explored. The volcano has a density of 3200 kg/m^3 , and elastic parameters Young's modulus 50 GPa and Poisson's ratio 0.3. The elastic lithosphere has a thickness of 90 km, a density of 3000 kg/m^3 , and elastic parameters Young's modulus 50 GPa and Poisson's ratio 0.3. The mantle has a density of 3500 kg/m^3 , and elastic parameters Young's modulus 100 GPa and Poisson's ratio 0.5. The viscosity of the mantle is 1×10^{21} Pas leading to a Maxwell time of approximately 3×10^{10} s. Post-failure behavior of the volcano and plate was modeled with Mohr-Coulomb plasticity (friction angle 40° , dilation angle 10° , yield stress 60 MPa).

Volcanic spreading was realized with a frictional contact between volcano and ground characterized by

various coefficients of friction μ . Full coupling is given for the welded contact ($\mu = \text{infinite}$), whereas full decoupling is given for the frictionless contact ($\mu = 0$).

The left and right boundaries of the model are fixed in radial direction but free to move in vertical direction. The lower model boundary is fixed in vertical direction. Martian gravity (3.7 m/s^2) is the only load applied to the model. To account for buoyancy, elastic foundations were used at the density interfaces.

Results: After instantaneous volcano emplacement, the lithosphere and mantle behave initially elastic. Later on, the downward flexure of the lithosphere increases due to the viscous behavior of the mantle. After approximately 1 Ma, which is the time of mantle isostatic equilibrium for the chosen parameters, the maximum downward displacement of the volcano center is -18 km.

Deformation of the volcano is measured in terms of plastic strain, because high values of plastic strain are associated with shear zones and faulting. Various models reveal three regions prone to faulting (Fig. 1): the upper volcano flanks, the volcano-ground interface, and the lithosphere at the volcano front. For a similar set of models, these regions were already found by [11]. All models show flank-parallel compression and high values of plastic strain on the upper volcano flanks, the location of terraces at Olympus Mons [3]. However, for a decoupled volcano (low μ) this zone has a much smaller extent than for a coupled volcano (high μ). High values of plastic strain at the interface between volcano and ground, where the maximum compressive stress is vertical, are found only for very low μ . The faulting zone in the lithosphere at the volcano front is characterized by vertical intermediate or maximum compressive stress.

Radial spreading of the volcano with respect to the lithosphere is possible for the decoupled models. As a result, the radius of the cone increases to 402.4 km for $\mu = 0$. For $\mu = 0.1$ the radius increases to 401.6 km. For $\mu = 0.3$ or larger, the increase in volcano radius is negligible.

Conclusions: Combined models of lithospheric flexure and volcanic spreading are able to account for the terraces observed on the upper flanks of Olympus Mons. The formation of the circumferential scarp is probably connected to the combined effects of a thrust at the front of the decoupled volcano, which is a

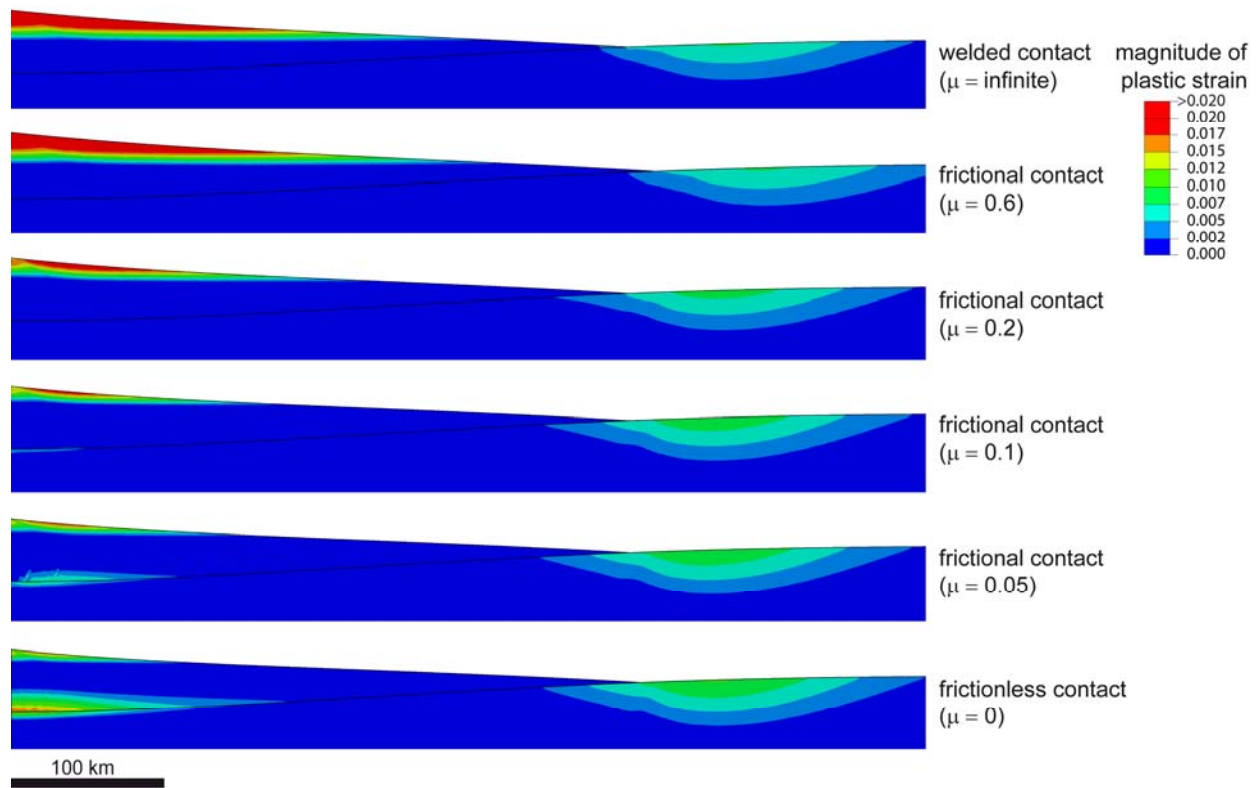


Figure 1. Plastic strain magnitudes for a radial section through axisymmetric model of Olympus Mons. The axis of rotation is to the left. Results are shown after mantle isostatic adjustment is complete (1 Ma). Solid line denotes volcano-ground interface with variable friction. No vertical exaggeration.

consequence of radial spreading, and the plastic deformation in the lithosphere at the volcano front.

However, models have to be refined and complemented in order to understand the formation of the scarp and aureole deposits.

Future Work: The assumption of an instantaneous load is valid if the growth time of the volcano is much smaller than the mantle Maxwell time. For the dimensions of Olympus Mons this would imply an eruption rate that is unrealistic high. Models including a growing volcano will lead to more realistic results. Further, lateral variations of the coupling between volcano and ground were not considered.

On Earth, volcanic scarps associated with massive landslides are known from the submarine parts of the Hawaiian and Canary Islands. [12] emphasizes the possibility that the scarp and aureole deposits of Olympus Mons formed under water. In this case, pore pressure and hydrothermal alteration would have influenced scarp and aureole formation.

References: [1] Plescia, J. B. (2004) *JGR*, 109, E03003. [2] Thomas, P. J. et al. (1990) *JGR*, 95, 14345-14355. [3] Byrne, P. K. et al. (2009) *EPSL*, 281, 1-13. [4] Watts, A. B. (2001) *Cambridge University Press*. [5] Jozwiak, L. M. et al. (2011) *LPSC XXXII*, Abstract #2202. [6] Borgia, A. et al. (1990) *JGR*, 95, 14357-14382. [7] Morris, E. C., and Tanaka, K. L. (1994) Geologic maps of the Olympus Mons Region of Mars, I2327. [8] Lopes, R. et al. (1982) *JGR*, 87, 9917-9928. [9] McGovern, P. J. et al. (2004) *JGR*, 109, E08008. [10] Shea, T. and van Wyk de Vries, B. (2008) *Geosphere*, 14, 657-686. [11] McGovern, P. J. and Solomon, S. C. (1993) *JGR*, 98, 23553-23579. [12] De Blasio, F. V. (2011) *EPSL*, 312, 23553-23579.